Dielectric recovery of an AC arc after current zero : Experimetal determination & simulation prediction

Thomas Merciris, Yann Cressault, Mathieu Masquère, Pascale Petit

DIELECTRIC RECOVERY OF AN AC ARC AFTER CURRENT ZERO: EXPERIMENTAL DETERMINATION & SIMULATION PREDICTION

T. MERCIRIS[12]*, Y. CRESSAULT[2], M. MASQUERE[2] AND P. PETIT[1]

[1]Schneider Electric, 31 Rue Pierre Mendès, 38158, Eybens, France
[2] Laboratoire Plasma et Conversion d'Energie (LAPLACE), Université de Toulouse, UPS, INPT
118 route de Narbonne, 31062, Toulouse, France
*thomas.merciris@se.com

ABSTRACT

This article studies the possibility to predict for which voltage a breakdown will take place in a post arc medium. We first measured experimentally the dielectric strength of a gap following an AC arc with silver electrodes and we developed a model based on a MHD simulation and the Boltzmann solver Bolsig+ to predict the post-arc dielectric strength.
Similar results between experimental and simulated breakdown voltages are obtained for a silver electrode after a 325A AC arc.

1. INTRODUCTION

Electric arcs in switching devices are studied and simulated since a long time, from academic to industrial perspectives and by different manufacturers (Schneider-Electric, Hager, ABB, …) but the goal stays the same in the breaking community: to better understand the current zero phase.

During the operation of a breaker, the device must stop the current flow by cooling down and extinguishing the arc initially created during the opening of the contacts. At the current zero (CZ), two processes are documented [1]:

1. The "thermal reignition" corresponding to a heating of the post-arc medium with a reconduction of current. This can be analysed through a Magneto-HydroDynamic (MHD) simulation of the plasma coupled to the electric network with a system of ordinary differential equations.
2. The second one corresponds to "dielectric reignition" due to the apparition of the transient recovery voltage (TRV). The hot dielectric gas between the contacts needs to withstand the TRV applied [2].

Recently, Lindmayer [3] published a model on this second process, the dielectric recovery using the model of Schmelzle for a sub-millimeter gap and a post dielectric strength after current interruption.

In this work we try to estimate the validity of this model on longer arcs with direct comparison with experimental data with pure silver electrode and explore the effect of the metallic vapours on the dielectric strength by the Townsend coefficients calculated with Bolsig+.

2. EXPERIMENTAL SETUP

In order to determine the post-arc dielectric strength experimentally, we developed a set-up according to similar research [4], that can generate an 8ms electric arc with variable current amplitudes (100A – 2kA) followed by an inverted voltage pulse, in order to reproduce the effect of a TRV with a variable amplitude (10 – 1kV) and variable delay after CZ.

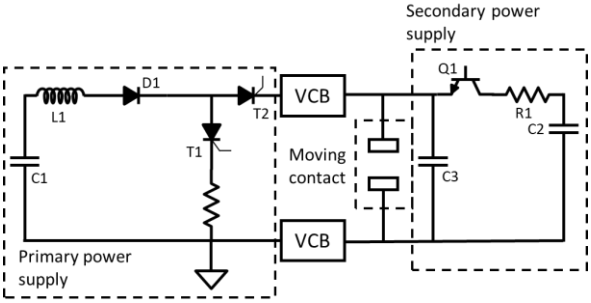

Fig. 1: Experimental setup

The primary power supply is composed of an LC resonating circuit triggered by SRCs. The voltage pulse is generated from a charged capacitance and a high voltage IGBT. The two voltages sources are isolated thanks to a Schneider Electric vacuum circuit breaker (VCB). The electrodes are made in pure silver and the opening of contacts is done with a LC1F265 contactor from Schneider Electric.

According to the work of [5], a statistical approach was implemented to estimate the 50%

probability of a dielectric breakdown at a given time after CZ.

3. MHD SIMULATION

We developed the MHD simulation, assuming a 2D axis-symmetric geometry to replicate the experimental setup presented above. We used ANSYS Fluent 2022 R2 to solve the fluid equations. The addition of the magnetic field's calculation and the Poisson equation is done via UDF. More information on the MHD model can be found on [6].

Dry air is used in this work and corresponding thermos-physical data comes from Cressault [7]. For the root modelling, the model of Mutzke was used [8] with modifications given in [9].

The heat equation is also solved in the solid part: the Murphy & Good law is used as sources term for thermoelectric losses on the cathode with the estimation of the root electric field form [10], model of Langmuir [11] for vaporization, and a blackbody for the radiation losses on the anode and cathode.

The dynamic of the contacts is modelized with a dynamic mesh using the measured experimental velocity of the mobile contacts. The initial electrode gap is 1mm and is initialised without movement during 3.3ms, with a Gaussian profile of 20kK, and a radius of 1mm. The mesh size was fixed at 25 µm between the electrodes using mix cartesian elements. The time step is fixed at 1µs with a total computation time of 48 hours.

4. DIELECTRIC MODELING

For the dielectric calculation, we can consider two cases: the streamer breakdown and the Paschen breakdown. For this work, the streamer regime is not happening in our case; the electron avalanche is not large enough to be self-sustainable. For the Paschen breakdown, the dielectric strength was calculated using the expression given by [12]:

$$\int_0^d \alpha(x) - \eta(x)\, dx = \ln\left(\frac{\gamma+1}{\gamma+\frac{J_t}{J}}\right) \qquad (1)$$

The ionization (α) and recombination (η) coefficients are deduced from the freeware Bolsig+, the gas composition and the cross-sections for air constituents available on the LxCat website [13]. J_t is the thermoelectric emission and J the total current computed in [12].

Those coefficients are dependent on the local temperature and the local electric field. We supposed here that the breakdown could happen between the two electrodes on the symmetry axis of the MHD simulation computed with dry air. The 1D temperature profile is then extracted. The influence on the dielectric strength of metallic vapor is computed considering 1% of Ag vapor in the gas composition without any modification on the previous temperature profile computed. For the silver constituents in the gas phase (Ag & Ag_2) the cross sections can be found from the theoretical calculations of [14] and [15]. The local electric field can be computed considering two cases:

(M1) with a cathode sheath composed of ions like in [3], where the plasma is not conductive on the cathode side and the electric field is neglected at the anode side. The local electric field is then given by equation (2):

$$E(x) = \frac{-3V_0}{2d}\sqrt{1-\frac{x}{d}} \qquad (2)$$

(M2) with a constant electric field on all the dielectric zone on the cathode and anode side. (no charge in the sheath).

These two cases need the identification of the nonconductive zones which is given by the temperature (T_crit) below for which the ionization degree of the plasma is below 0.1%. An example of the temperature profile is given on figure 2:

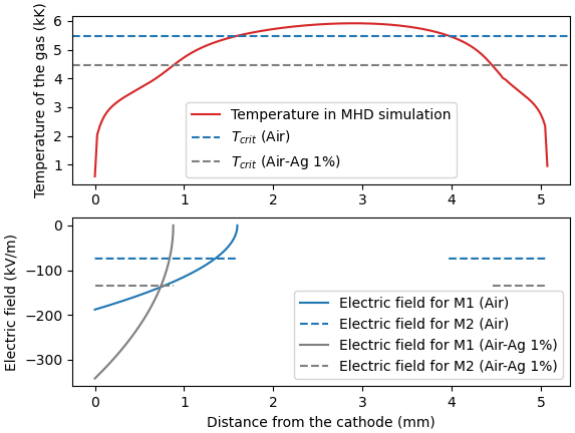

Fig. 2: a) Temperature profile on the symmetric axis at t = 9 ms, b) The electric field estimation with the two methods for V_0 = 200V.

4. RESULTS

From the experimental setup, the probability curves for each Δt after CZ are obtained with their relative uncertainties. The extinction probability

in function of the applied voltage for multiple delay after CZ is plotted on figure 3.

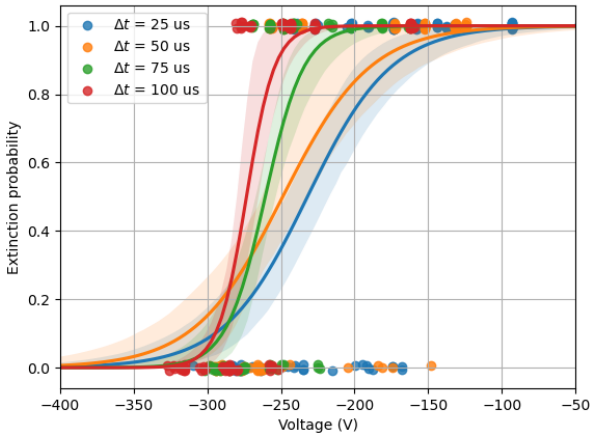

Fig. 3: Extinction probability vs applied voltage for 25, 50, 75 and 100µs after CZ

A large dispersion of the breakdown voltage (about 100V) is observed.

From the MHD simulation, on figure 4, we compared the simulated and measured arc voltages. A small variation from the experimental result is observed, maybe due to the precision on the contact velocity.

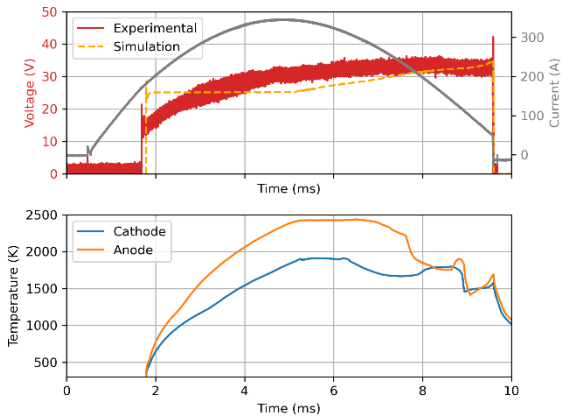

Fig.4: a) Current & arc voltage in the experimental setup & in the simulation. b) Maximum electrodes temperature in the simulation

The electrodes temperature is also monitored, with the maximum temperature at the anode and cathode in function of time. We observe a sharp decrease of the electrodes temperature after the arc extinguish.

From the Bolsig+ calculation, we compute the critical electric field ($\alpha(E,T) - \eta(E,T) = 0$) in presence of silver vapors (Fig.5). We did not find any previous works using silver vapors, but numerous works exist with copper vapors. Our results are similar to the work of Tanaka [16].

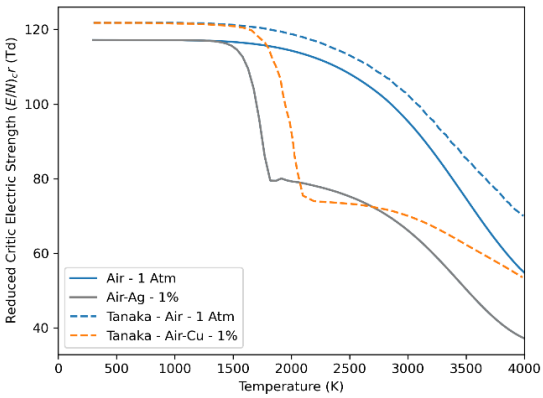

Fig. 5: Reduced critical electric field for Air & Air-Ag mixture (1% Molar). Comparison with the result of Tanaka [16]

Figure 6 highlights the result of electric fields for the two cases (M1 & M2) by equation 1, in pure air or mixed with 1% of metallic vapor. The experimental value obtained for dielectric strength is also reported. (Extinction probability of 50% - Fig 3)

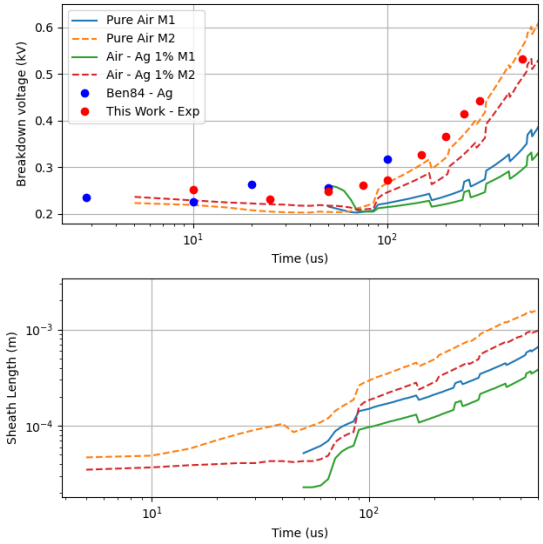

Fig. 6: a) Dielectric strength of the post-arc medium obtained from model with pure air and air-ag mixture (1%) and from experimental measurement. b) Sheath size estimation with the different models.

We can observe that the evolution of the breakdown voltage is keep stable during the first 0.1ms of the dielectric recovery around 250V and then increases rapidly. This agrees with the work of [12]. Very close simulation results to the experimental data will be also presented and tend to validate this model.

5. DISCUSSION

On the critical electric field, we did observe some variation between our work and [16]. The variation in critical electric field at 300K can be easily explained by the variation of cross sections

used in this work. The temperature shift is caused by the lower vaporization point of silver compared to copper with a shift about 400K.

Experimentally, we found the same dielectric recovery as [12] for the silver electrodes. The experimental procedure was a bit different; we did not polish the electrode after each run, one can suppose that the state of the electrode after the arc is molten with very few sharp imperfections. The field emission is thus not amplified by the surface rugosity.

The different mode of calculation of the dielectric distance gave similar results at 100µs after CZ but began to diverge as the time increase. This is cause by the dielectric gap at the anode that is not considered in M1. However, in low voltage breaking most TRV are below this order of time after CZ.

We observed that the addition of metallic vapor lowers the dielectric strength, this is explained by an ionization coefficient higher and a shorter dielectric length due to the lowering of T_{crit}. This is the principal limit on this model, we did not simulate the metallic vapor profile in the MHD simulation: the thermodynamic property will change and so will the temperature profile on the dielectric calculation. (Fig.2)

We "fixed" the path of the breakdown on our setup, but in a 3D breaking device, the problem is more complex. An idea is to find the path that minimize the breakdown voltage with an optimization algorithm.

6. CONCLUSION

A complete model of the post-arc medium was developed with the objective of predicting the dielectric strength after the arc phase. Our results are very close to the experimental data presented here and with previous work for a stationary arc.

This is a preliminary result and need to be extended to a moving arc and a complex geometry to be useful in the prediction of circuit breakers performance.

REFERENCES

[1] Reichert, F et al. *Modelling and Simulation of SF6 High-Voltage Circuit-Breakers - an Overview on Basics and Application of CFD Arc Simulation Tools.* Plasma Physics and Technology **4**, 213–224 (2017).

[2] Slepian, J. *Extinction of a Long A-C. Arc*. Transactions of the American Institute of Electrical Engineers **49**, 421–430 (1930).

[3] Lindmayer, M. *Recovery of Short AC Switching Arcs - An Old Principle Newly Investigated.* 30th International Conference on Electrical Contact (2021).

[4] Shea, J. J. *The influence of arc chamber wall material on arc gap dielectric recovery voltage. in Electrical Contacts*. 46th IEEE Holm Conference on Electrical Contacts 161–168 (2000).

[5] Bösche, D et al. *Investigating of the Recovery Behaviour of a Small Switching Gap after Current Interuption*. Plasma Physics and Technology **4**, 165–168 (2017).

[6] Freton, P. et al, *Magnetic field approaches in dc thermal plasma modelling*. J. Phys. D: Appl. Phys. **44**, 345202 (2011).

[7] Cressault, Y. et al. *Influence of metallic vapours on the properties of air thermal plasmas.* Plasma Sources Sci. Technol. **17**, 035016 (2008).

[8] Mutzke, A. et al. *Modeling the Arc Splitting Process in Low-Voltage Arc Chutes*. 53rd IEEE Holm Conference on Electrical Contacts 175–182 (2007).

[9] Shin, D. et al. *Arc Modeling to Predict Arc Extinction in Low-Voltage Switching Devices.* IEEE Holm Conference on Electrical Contacts 222–228 (2018).

[10] Mackeown, S. S. *The Cathode Drop in an Electric Arc*. Phys. Rev. **34**, 611–614 (1929).

[11] I. Langmuir, *The adsorption of gases on plane surfaces of glass, mica and platinum*, Journal of American Chemical Society **40**, 1361, 1918.

[12] Bentounes, H. A. *Influence de la nature des électrodes sur la vitesse de rétablissement de la rigidité diélectrique d'un millieu post-arc.* Université de Paris-Sud (1984).

[13] E. Carbone et al. *Data Needs for Modeling Low-Temperature Non-Equilibrium Plasmas: The LXCat Project, History, Perspectives and a Tutorial*. Atoms **9** (1), 16. (2021)

[14] McNamara, K. et al. *Calculation of electron scattering on atomic silver.* J. Phys. B: At. Mol. Opt. Phys. **51**, 085203 (2018).

[15] Deutsch, H. et al. *Theoretical determination of the absolute electron impact ionization cross-section function for silver clusters Agn (n=2–7).* J. Chem. Phys. **111**, 1964–1971 (1999).

[16] Tanaka, Y. *Influence of copper vapor contamination on dielectric properties of hot air at 300-3500 K in atmospheric pressure.* IEEE Transactions on Dielectrics and Electrical Insulation **12**, 504–512 (2005).